1008 *Inorg. Chem.* **2010**, *49*, 1008–1016
DOI: 10.1021/ic901813t

Inorganic Chemistry
Article

Mechanism of Ionic Recognition by Polymer-Supported Reagents: Immobilized Tetramethylmalonamide and the Complexation of Lanthanide Ions

Yijia Yang and Spiro D. Alexandratos*

Department of Chemistry, Hunter College of the City University of New York, 695 Park Avenue, New York, New York 10065

Received September 11, 2009

The mechanism of ionic recognition by polymer-supported reagents is probed with cross-linked polystyrene modified with tetramethylmalonamide (TMMA) ligands. The substrates are lanthanide ions in 0.001−8 M HCl and HNO_3 solutions. The results fall into three regions of acid concentration: low, mid, and high. In HCl, distribution coefficients are low in 0.001 to 2 M, increase in 4 and 6 M, and then decrease in 8 M HCl. In the low-acid region, the metal ion remains with its waters of hydration and does not coordinate to the carbonyl oxygens. As the acid concentration exceeds 2 M, protonation of the amide occurs to form an iminium moiety, electrostatically attracting the anionic lanthanide complex through ion-exchange and releasing waters of hydration. At high acid concentration, the apparent affinity decreases due to competition by the large excess of chloride ions for the ion-exchange sites. The affinity sequence in 6 M HCl is Tb > Dy > Eu > Gd > Ho > Sm > Er > Tm > Yb > Lu > Nd > Ce > La. The TMMA−Ln interaction is due to *recognition* since there is a point of maximum affinity across the series rather than a monotonic trend. The trends are comparable in HNO_3. A comparison of the distribution coefficients at the maxima (6 M HCl and 4 M HNO_3) shows nitrate to have greater values than chloride due to a hydration effect, as also indicated by results from H_2SO_4.

Introduction

Ionic recognition is a concept with important fundamental and technological implications. In biology, ionic recognition in peptides can depend on as little as one change in the amino acid sequence.[1] With low molecular weight compounds, the interaction of metals with crown ethers is perhaps the most prevalent example of ionic recognition,[2] but other important examples involve calixarenes,[3] cryptands,[4] and fulvalenes.[5] Ionic recognition has been applied to ion-selective electrodes,[6] sensors,[7] and environmental remediation.[8] The concept has been extrapolated to cross-linked polymers by modifying them with crown ethers[9] and calixarenes[10] as well as by imprinting size selectivity onto them.[11]

Cross-linked polymers with functional groups capable of binding metal ions offer advantages that include ease of operation, regeneration and reuse, and environmental compatibility.[12] These properties are important to numerous applications, including catalysis,[13] chromatography,[14] and the separation of toxic metals from waste solutions[15] and water in the environment.[16] An understanding of selectivity in the immobilized ligand−metal ion interaction is important to these applications.

This report is part of our broader study into the mechanism of metal ion complexation by polymer-supported reagents with the objective of understanding the conditions required for ionic recognition to occur.[17]

N,*N*,*N*′,*N*′-Tetramethylmalonamide (TMMA) is the ligand chosen for this initial study. The metal ion affinities of the soluble analogues can be varied with alkyl groups: linear

*Corresponding author. E-mail: alexsd@hunter.cuny.edu.

(1) Matzapetakis, M.; Pecoraro, V. L. *J. Am. Chem. Soc.* **2005**, *127*, 18229–18233.
(2) Bradshaw, J. S.; Izatt, R. M.; Savage, P. B.; Bruening, R. L.; Krakowiak, K. E. *Supramolec. Chem.* **2000**, *12*, 23–26.
(3) Casnati, A.; Sansone, F.; Ungaro, R. *Adv. Supramolec. Chem.* **2003**, *9*, 163–218.
(4) Menon, S. K.; Hirpara, S. V.; Harikrishnan, U. *Rev. Anal. Chem.* **2004**, *23*, 233–267.
(5) Trippe, G.; Levillain, E.; Le Derf, F.; Gorgues, A.; Salle, M.; Jeppesen, J. O.; Nielsen, K.; Becher, J. *Org. Lett.* **2002**, *4*, 2461–2464.
(6) Shishkanova, T. V.; Sapurina, I.; Stejskal, J.; Kral, V.; Volf, R. *Anal. Chim. Acta* **2005**, *553*, 160–168.
(7) Gupta, V. K.; Ludwig, R.; Agarwal, S. *Anal. Chim. Acta* **2005**, *538*, 213–218.
(8) de Gyves, J.; de Miguel, E. R. *Ind. Eng. Chem. Res.* **1999**, *38*, 2182–2202.
(9) Gibson, H. W.; Ge, Z.; Huang, F.; Jones, J. W.; Lefebvre, H.; Vergne, M. J.; Hercules, D. M. *Macromolecules* **2005**, *38*, 2626–2637.
(10) Alexandratos, S. D.; Natesan, S. *Macromolecules* **2001**, *34*, 206–210.
(11) Maeda, M.; Bartsch, R. A. *ACS Symp. Ser.* **1998**, *703*, 1–8.
(12) Sherrington, D. C.; Hodge, P. *Syntheses and separations using functional polymers*; John Wiley & Sons: Chichester, UK, 1988; p 454.
(13) Sherrington, D. C. Polymer-supported transition metal complex alkene epoxidation catalysts. *Supported Reagents and Catalysts in Chemistry*; Royal Society of Chemistry: London, 1998, Vol. *216*, pp 220−228.
(14) Shaw, M. J.; Cowan, J.; Jones, P. *Anal. Lett.* **2003**, *36*, 423–439.
(15) Zhu, Y.; Millan, E.; Sengupta, A. K. *React. Poly.* **1990**, *13*, 241–53.
(16) Seko, N.; Tamada, M.; Yoshii, F. *Nucl. Instrum. Methods Phys. Res.* **2005**, *236*, 21–29.
(17) Alexandratos, S. D.; Zhu, X. *Macromolecules* **2005**, *38*, 5981–5986.

Published on Web 01/05/2010

dialkylamides can be used for the recovery of Pu while branched chain dialkyl amides are good extractants for U(VI).[18] Amides are an alternative to organophosphorus extractants for the separation of lanthanides and actinides from nuclear fuel reprocessing streams.[19] They can also be bonded to polymers: TMMA has been immobilized[20,21] and has high affinities for U(VI) and Ce(III), 4-ethoxy-*N*,*N*-dihexylbutanamide is selective for U(VI), Th(IV), La(III), and Nd(III) from acidic solutions, and di-bis(2-ethylhexyl)-malonamide extracts U(VI) from up to 4 M acid.[22]

In the current study, the affinities of the diamide for the lanthanides were determined because of their monotonically varying properties (ionic radius, charge density, hydration enthalpy, etc.), similar complex geometries, and polarizabilities that vary over a narrow range of hardness. Covalent interactions are minimal since the f-orbitals being populated are not the outermost orbitals.[23] The design of polymer-supported reagents which allow for the selective complexation of lanthanide ions from aqueous solutions is important in its own right due to applications in nuclear waste management,[24] luminescent probes,[25] and catalysis.[26]

Experimental Section

Materials. TMMA was purchased from TCI America. All other chemicals were obtained from Sigma-Aldrich or Acros and used without further purification unless otherwise noted. The preparation of the cross-linked poly(vinylbenzyl chloride) beads has been described[27] and is summarized below. The beads had a particle size of 0.25−0.42 mm. Reactions at other than room temperature or reflux were regulated with a Therm-O-Watch temperature control device. Water for metal ion studies and analytical determinations was filtered through a Millipore Direct Q-5 system and had a resistivity of 18.2 MΩ cm.

Synthesis of Poly(vinylbenzyl chloride) Cross-Linked with 2% Divinylbenzene. The poly(vinylbenzyl chloride) gel copolymer was prepared by suspension polymerization of vinylbenzyl chloride (VBC) and 2 wt % divinylbenzene (DVB).[27] The aqueous phase, prepared by dissolving 1.25 g of polyvinyl alcohol and 28.0 g of calcium chloride in 250 mL water, was poured into a 1 L three-neck round-bottom flask fitted with condenser, nitrogen inlet, thermometer, and overhead digital stirrer and sparged 10 min with nitrogen. The organic phase of 143.08 g VBC, 5.42 g DVB (55.4% purity), and 1.50 g benzoyl peroxide (BPO), was sparged with nitrogen for 5 min after being mixed thoroughly and then added to the flask containing the aqueous phase under a nitrogen sweep.

The reaction was heated at 80 °C for 10 h, and the polymerization completed by a 2-h reflux after adding 100 mL water. The beads were washed with 10^{-4} M aqueous HCl once and with water three times, Büchner-dried, and extracted with toluene for 17 h. After extraction, the beads were dried and sieved using US standard screens.

Table 1. Poly(VBC-co-MMA)-Bound TMMA Components

VBC/MMA (mol/mol)	wt_{beads} (g)	wt_{NaH} (g)	wt_{TMMA} (g)
80/20	2.5	2.3	9.50
50/50	1.0	0.70	2.75
20/80	1.9	0.43	1.70

Synthesis of Macroporous PolyVBC Beads Cross-Linked with 5% DVB. Macroporous beads were prepared by suspension polymerization of VBC, 5 wt % DVB, 1 wt % BPO, and 50 vol% 4-methyl-2-pentanol as the porogen.

Synthesis of Poly(VBC-co-MMA) Cross-Linked with 2% DVB. Poly(VBC-co-methyl methacrylate) was prepared by suspension polymerization of VBC, methyl methacrylate (MMA), 2 wt % DVB, and 1 wt % BPO. The molar ratios of VBC to MMA were 80/20, 50/50, and 20/80. After polymerization, the beads were washed with distilled water and extracted with toluene.

Synthesis of PolyVBC-bound *N*,*N*,*N*′,*N*′-Tetramethylmalonamide (TMMA). TMMA (9.5 g, 60 mmol) was dissolved in 100 mL of 1-methyl-2-pyrrolidone (NMP), and 2.3 g of NaH (60% dispersion, 57 mmol) was added in portions. After the reaction mixture was heated at 60 °C for 2 h, 2.0 g of polyVBC beads swollen in 50 mL of NMP were added and the reaction was stirred at 80 °C for 17 h. The beads were recovered and washed with NMP and water, placed in a glass frit funnel, and conditioned with 1 L each of H_2O, 1 M NaOH, H_2O, 1 M HCl, and H_2O.

Synthesis of PolyVBC-Bound Diethylmalonate. Diethylmalonate (9.1 mL, 60 mmol) was dissolved in 100 mL NMP and 2.3 g of NaH (60% dispersion, 57 mmol) was added in portions. The reaction mixture was heated at 60 °C for 2 h, 2.0 g of polyVBC beads swollen in 50 mL of NMP were added, and the reaction was stirred at 80 °C for 17 h. The beads were recovered and treated as above.

Synthesis of Poly(VBC-co-MMA)-Bound TMMA. The polymer with TMMA bound to poly(VBC-co-MMA) was prepared by the reaction of TMMA and poly(VBC-co-MMA) in a manner similar to the preparation of polyVBC-bound TMMA. TMMA was dissolved in 100 mL of NMP and NaH (60% dispersion) then added in portions. The amount of each reactant was calculated to give a $-CH_2Cl$:NaH:TMMA ratio of 1:5:5 (Table 1). After the mixture was heated at 60 °C for 2 h, 2.0 g of poly(VBC-co-MMA) swollen in 50 mL of NMP were added and the reaction was stirred at 80 °C for 17 h. The beads were recovered and treated as above.

Synthesis of Polystyrene-Bound Amide. PolyVBC beads (10 g) were added to a reaction flask containing 30 g $NaHCO_3$ and 150 mL DMSO, and the mixture refluxed for 20 h. After washing with ethanol, the beads were contacted with 60 mL of dioxane for 1 h, refluxed for 24 h after the addition of 130 mL of 3 M HNO_3, washed with water, dried and contacted with 60 mL of dioxane for 17 h followed by a 24-h reflux after the addition of 130 mL of 30% H_2O_2 to give a resin functionalized with −COOH groups. Amidation was completed by refluxing 2.0 g

(18) (a) Patil, C. B.; Mohapatra, P. K.; Singh, R. R.; Gurba, P. B.; Janardan, P.; Changrani, R. D.; Manchanda, V. K. *Radiochim. Acta* **2006**, *94*, 331–334. (b) Manchanda, V. K.; Ruikar, P. B.; Sriram, S.; Nagar, M. S.; Pathak, P. N.; Gupta, K. K.; Singh, R. K.; Chitnis, R. R.; Dhami, P. S.; Ramanujam, A. *Nucl. Tech.* **2001**, *134*, 231–240. (c) Ruikar, P. B.; Nagar, M. S.; Subramanian, M. S.; Gupta, K. K.; Varadarajan, N.; Singh, R. K. *J. Radioanal. Nucl. Chem.* **1995**, *196*, 125–134. (d) Pathak, P. N.; Veeraraghavan, R.; Prabhu, D. R.; Mahajan, G. R.; Manchanda, V. K. *Sep. Sci. Technol.* **1999**, *34*, 2601–2614.

(19) (a) Condamine, N.; Musikas, C. *Solv. Extr. Ion Exch.* **1992**, *10*, 69–100. (b) Gupta, K. K.; Manchanda, V. K.; Subramanian, M. S.; Singh, R. K. *Solv. Extr. Ion. Exch.* **2000**, *18*, 273–292. (c) Mahajan, G. R.; Prabhu, D. R.; Manchanda, V. K.; Badheka, L. P. *Waste Management* **1998**, *18*, 125–133. (d) Manchanda, V. K.; Pathak, P. N. *Separ. Purif. Tech.* **2004**, *35*, 85–103. (e) Byers, P.; Drew, M. G. B.; Hudson, M. J.; Isaacs, N. S. *Polyhedron* **1994**, *13*, 349–352.

(20) Nogami, M.; Ismail, I. M.; Yamaguchi, M.; Suzuki, K. *J. Solid State Chem.* **2003**, *171*, 353–357.

(21) Ismail, I. M.; Nogami, M.; Suzuki, K. *Sep. Purif. Tech.* **2003**, *31*, 231–239.

(22) Pranhakaran, D.; Subramanian, M. S. *Talanta* **2005**, *65*, 179–184.

(23) Carlos, L. D.; Malta, O. L.; Albuquerque, R. Q. A covalent fraction model for lanthanide compounds. *Chem. Phys. Lett.* **2005**, *415*, 238−242.

(24) Gruener, B.; Plesek, J.; Baca, J.; Cisarova, I.; Dozol, J. F.; Rouquette, H.; Vinas, C.; Selucky, P.; Rais, J. *New J. Chem.* **2002**, *26*, 1519–1527.

(25) Hemmilae, I.; Laitala, V. *J. Fluoresc.* **2005**, *15*, 529–542.

(26) Hultzsch, K. C.; Gribkov, D. V.; Hampel, F. *J. Organomet. Chem.* **2005**, *690*, 4441–4452.

(27) Beauvais, R. A. *Synthesis and characterization of interpenetrating polymer network resins, polymer foam-supported ligands, and polystyrene/polyphenolic ion-complexing reagents.* Ph.D. Dissertation, University of Tennessee, Knoxville, **1997**.

Scheme 1. Synthesis of Polystyrene-Bound TMMA

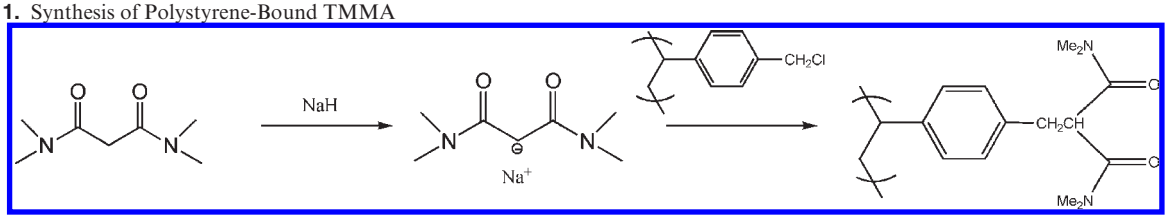

Table 2. Characterization of Polystyrene-Bound Gel Resins

functional group	% solids	Cl capacity (mmol/g)	N capacity (mmol/g)
chloromethyl	78.8	5.79	
monoamide	57.7	1.11	2.93
malonate diester	72.1	1.24	
TMMA	41.1	0	6.26

of vacuum-dried carboxylic acid resin in 100 mL of $SOCl_2$ for 48 h, followed by the addition of 30 mL of 2 M solution of dimethylamine in tetrahydrofuran (THF) after removing excess $SOCl_2$. The mixture was stirred at 45 °C for 17 h. The beads were recovered, washed with THF and water, placed in a glass frit funnel, and conditioned with 1 L each of H_2O, 1 M NaOH, H_2O, 1 M HCl, and H_2O.

Characterization of Functionalized Resins. The resins were characterized by their percent solids, acid capacity, chlorine capacity, nitrogen capacity, and FTIR spectrum.[27] The spectra were obtained on a Bomem MB Series FTIR in which KBr pellets were prepared with 0.01 g of resin and 0.100 g of KBr followed by grinding and compression into pellets.

Metal Ion Study. Resin (0.10 g) was contacted with 5 mL of 10^{-4} N solutions of the metal ions for 17 h on a digital orbital shaker (VWR, DS-500) at a speed of 200 rpm. Each resin was pre-equilibrated with a solution of HCl, HNO_3, or H_2SO_4 of the same acidity as the metal-containing solution. The amount of metal complexed was determined with an inductively coupled plasma−atomic emission spectrometer (Spectroflame M 120E).

Results

TMMA was bonded to polyVBC via nucleophilic addition as shown in Scheme 1. The synthesis consisted of deprotonating TMMA with NaH and nucleophilic addition. NMP was chosen as solvent because it dissolves the sodium salt.

The gel resins are characterized in Table 2. (Each resin was prepared numerous times in order to establish reproducibility of the synthesis.) Comparing the experimental to the theoretical values (5.12 and 7.19 mmol/g for the monoamide and diamide, respectively), the degrees of functionalization are calculated to be 80% for the diester, 60% for the monoamide, and >85% for the diamide. Based on the chlorine capacity, the diester is 80% functionalized. The decreasing solid levels from polyVBC to the diester and diamide resins is due to the increasing hydrophilicity of the $-CH_2Cl$, $-C(O)OEt$, and $-C(O)NMe_2$ moieties.

The malonamide ligand was immobilized onto macroporous polyVBC. The degree of functionalization for the TMMA resin is >98%, as calculated from its nitrogen capacity of 5.97 mmol/g (complete functionalization yields 6.06 mmol/g).

The density of the TMMA groups on the polymer backbone was altered by anchoring TMMA onto copolymers with VBC/MMA molar ratios of 100/0, 80/20, 50/50, and 20/80. Since TMMA can react only with the VBC moiety, the decreasing VBC content on the polymer from 100% to 80%, 50%, and 20% (chlorine capacities of 5.79, 4.40, 3.22, and 1.12 mmol/g, respectively) leads to the decrease in TMMA on the resin (nitrogen capacities of 6.26, 5.12, 3.60, and 2.04 mmol/g, respectively).

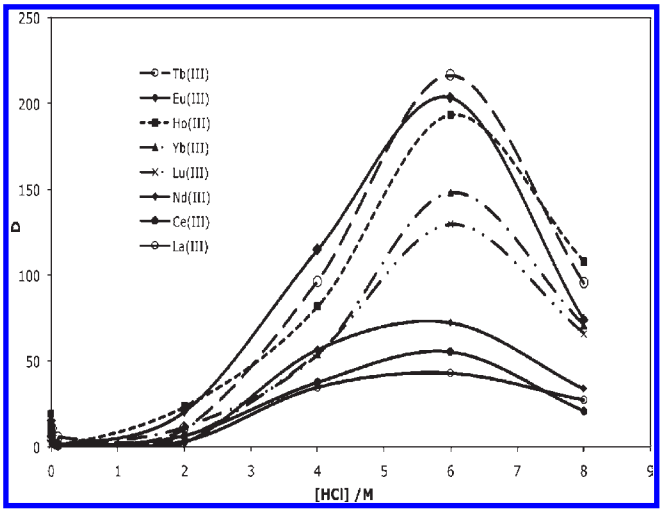

Figure 1. Distribution coefficients of the lanthanides at varying HCl concentration.

The FTIR spectra show the characteristic bands for polyVBC including strong bands at 1265 cm^{-1} due to C—H symmetric bending of the CH_2—Cl group and 708 cm^{-1} due to C—Cl stretching. The diester resin shows a strong band at 1734 cm^{-1} due to the carbonyl stretch and 1180 cm^{-1} due to C—O—C symmetric and asymmetric stretching. The TMMA and monoamide resins show amide C=O stretching bands at 1649 and 1637 cm^{-1}, respectively.

The nitrogen capacities of the TMMA and monoamide resins were determined before and after the resins were shaken in 8 M HCl and 8 M HNO_3 for 17 h. The values were unchanged, indicating that the resins are stable under highly acidic conditions.

Effect of HCl Concentration on Lanthanide Affinities. The lanthanide affinities for the diamide resin were determined as a function of HCl concentration (Figure 1): the distribution coefficients are low from 0.001 to 2 M HCl, increase in 4 and 6 M HCl, then decrease as the HCl concentration increases to 8 M. The highest affinities are seen for Tb, Eu, and Ho, and this is more pronounced in 4 and 6 M HCl (Figure 2).

Comparative Study of the Monoamide, Diamide, and Diester Resins in HCl. A comparative study was conducted by contacting the monoamide, diamide, and diester resins with 10^{-4} N solutions of the lanthanide ions in 4 and 6 M HCl (Table 3). The metal ion affinities were quantified in terms of the distribution coefficients and percent sorption. The monoamide resin had only low affinities for the lanthanides from 4 and 6 M HCl while the diamide resin had significant affinity. The diester resin

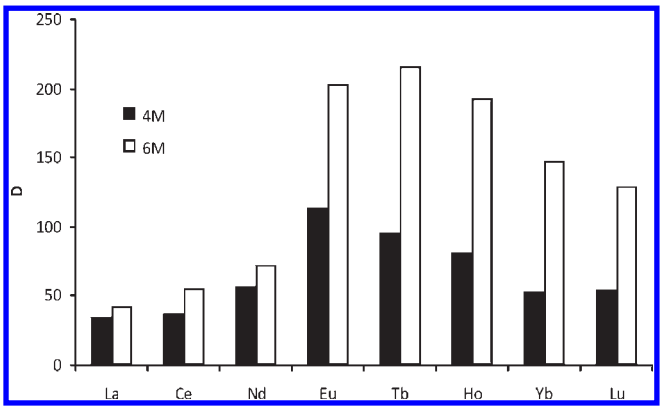

Figure 2. Distribution coefficients of the lanthanides from 4 and 6 M HCl.

had no affinity for La, Eu, and Lu from 4 M HCl and a low affinity from 6 M HCl.

Effect of Ligand−Ligand Interaction: VBC-co-MMA Copolymers in HCl. In order to evaluate the possibility of interligand cooperation in the binding of a given lanthanide, the TMMA ligands were separated by ester groups through the covalent attachment of TMMA onto VBC-co-MMA polymers with varying VBC/MMA molar ratios (100/0, 80/20, 50/50, and 20/80). Decreasing *D* with decreasing TMMA content on the polymer from 100% to 80%, 50%, and 20% is observed when the distribution coefficients are calculated on a per gram resin basis (Figure 3A). However, when the distribution coefficients are recalculated on a per millimole ligand basis (*D*'), no significant difference in affinities is found among the 100%, 80%, and 50%-functionalized resins (Figure 3B). Lower affinities are evident only for Eu, Tb, Ho, and Yb with the 20%-functionalized resin. The interaction thus occurring between the TMMA ligand and the lanthanide complex may be ascribed to a single ligand.

Affinity Sequence in 6 M HCl with the Macroporous Resin. The affinity series with the microporous (gel) TMMA resin from 6 M HCl is Tb > Eu > Ho > Yb > Lu > Nd > Ce > La. In order to determine whether the distribution coefficients are affected by accessibility of the ions into the polymer, the results from the gel resin were compared to those from a macroporous resin (Figure 4). Both resins give a similar sequence, though the difference of Tb > Eu > Ho in the gel resin is more like Eu > Tb > Ho in the macroporous resin. Additionally, there are slightly higher distribution coefficients with the macroporous resin for almost all lanthanides, though these differences are small except for Eu.

Complete Lanthanide Series in HCl. Complexation of the lanthanides by TMMA was extended to the complete series (excluding Pr (due to analytical difficulties with the ICP) and Pm (due to its radioactivity)) from 6 M HCl (Figure 5). Each run was repeated six times. The distribution coefficient increases gradually from La to Nd, jumps to a level twice as much as that at Nd for Sm and Eu, and decreases at Gd. It rebounds to a new high at Tb and gradually decreases for Dy and Ho. After that, the distribution coefficient declines slowly toward Lu. In general, the trend remains the same as that observed earlier for the seven lanthanides—*D* values increase from La to Tb and decrease from Tb to Lu. According to the average *D* values, the series can be divided into four subgroups by breakpoints at Sm, Gd, and Er (La → Nd(Pm), Sm → Gd, Gd → Ho, and Er → Lu). This variation of affinities is consistent with the "gadolinium break" or "three-quarter shell effect" reported with soluble complexants,[28] including di-*n*-octylphosphinic acid and di-2-ethylhexylchloromethylphosphonate. This observation with immobilized ligands indicates that complexants could maintain their coordination properties after being immobilized onto polymer supports.

Effect of HNO_3 Concentration on Lanthanide Affinities. The HNO_3 concentration dependency exhibits a trend similar to that in HCl (Figure 6): distribution coefficients increase from 2 to 4 M then decrease as the acid concentration exceeds 5 M. The extraction of HNO_3 by soluble malonamide is significant when the concentration exceeds 2 M and increases with increasing acid concentration.[29] For most lanthanides (except Lu which has similar affinities in 4 and 6 M HNO_3), the highest affinities are from 4 M HNO_3 (Figure 7). The affinity sequence in 4 M HNO_3 follows the same pattern as that found in 6 M HCl with the affinities being higher for the lanthanides in the middle of the series than the ones at the two ends: Ho ≈ Yb ≈ Tb > Nd > Eu > Lu ≈ Ce > La.

Discussion

Effect of HCl Concentration on Lanthanide Affinities. The trends in Figures 1 and 2 show a maximum affinity toward the middle of the lanthanide series rather than a steadily increasing (or decreasing) affinity and this affinity is influenced by the HCl concentration. The results may be divided into three regions: low acid (0.001−2 M), midacid (4−6 M), and high acid (8 M).

In the low acid region, there is little sorption of the lanthanides because coordination by TMMA is weaker than binding by the waters of hydration (Scheme 2).

In the midacid region, there is significant sorption of the lanthanides from 6 M HCl with a maximum affinity toward the middle of the series. The protonation of soluble malonamide in 4 M HCl is confirmed by the ^{1}H NMR spectrum: a peak appearing at 5.3 ppm is assigned to the proton bound to the amide.[30] Protonation occurs at the carbonyl oxygen rather than the nitrogen to form a six-membered ring with the neighboring carbonyl group.[31,32] Consistent with this, we propose that as the HCl concentration exceeds 2 M, protonation of the amide occurs which is stabilized by hydrogen bonding to the adjacent carbonyl oxygen (no protonation occurs in the absence of the adjacent carbonyl). This protonation results in the formation of an iminium moiety (Scheme 3).

The iminium chloride is the site of ion exchange with the lanthanide chlorocomplex. The concentration of HCl

(28) (a) Sinha, P. S. *Helv. Chim. Acta* **1975**, *58*, 1978–1983. (b) Nugent, L. J. *J. Inorg. Nucl. Chem.* **1970**, *32*, 3485–3491. (c) Peppard, D. F.; Mason, G. W.; Lewey, S. *J. Inorg. Nucl. Chem.* **1969**, *31*, 2271–2272.
(29) Spjuth, L.; Liljenzin, O.; Skålberg, M.; Hudson, M. J.; Chan, G. Y. S.; Drew, M. G. B.; Feaviour, M.; Iveson, P. B.; Madic, C. *Radiochim. Acta* **1997**, *79*, 39–46.
(30) Costa, M. C.; Carvalho, A.; Uryga, A.; Paiva, A. P. *Solv. Extr. Ion Exch.* **2003**, *21*, 653–686.
(31) Musikas, C.; Hubert, H. *Solv. Extr. Ion Exch.* **1987**, *5*, 151–174.
(32) Nakamura, T.; Mikyake, C. *Solv. Extr. Ion Exch.* **1995**, *13*, 253–273.

Table 3. Distribution Coefficients and Percents Sorption of the Lanthanides Complexed by the Monoamide, Diamide, and Diester Resins from HCl Solutions

	monoamide				diamide				diester			
Ln(III)	4 M HCl		6 M HCl		4 M HCl		6 M HCl		4 M HCl		6 M HCl	
	D	% sorb	*D*	% sorb	*D*	% sorb	*D*	% sorb	*D*	% sorb	*D*	% sorb
La	0	0	10.9	8.2	34.4	23.2	42.9	24.2	0	0	16.8	24.0
Ce	5.7	4.7	4.9	4.1	37.4	24.4	55.2	30.3				
Nd	16.2	8.9	10.8	11.6	56.4	33.5	72.2	40.1				
Eu	0	0	21.2	15.8	114.6	49.3	203.3	63.0	6.0	4.9	22.1	33.2
Tb	0	0	2.1	1.8	96.5	45.5	216.2	65.1				
Ho	0	0	17.2	13.4	81.5	41.8	193.2	60.8				
Yb	1.5	1.2	23.1	16.2	53.7	32.0	148.0	51.9				
Lu	0	0	10.1	8.0	54.1	32.3	129.4	49.9	0	0	13.5	18.2

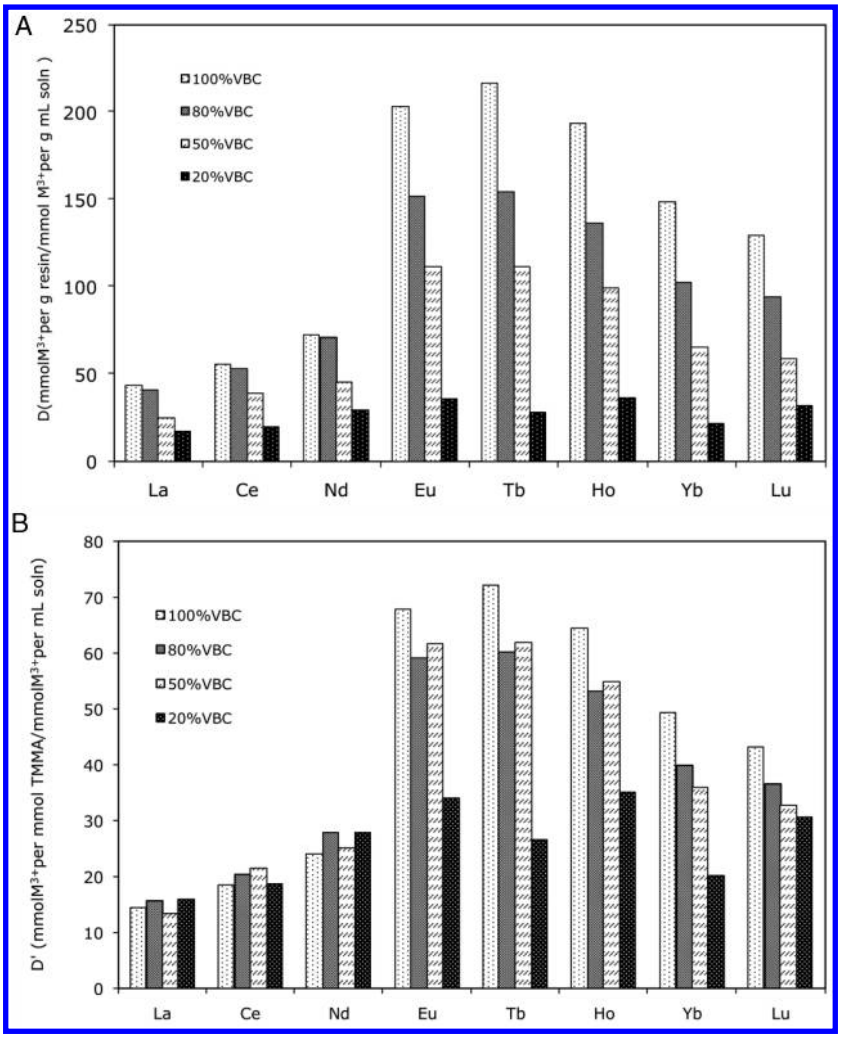

Figure 3. (A) Distribution coefficients of lanthanide ions in 6 M HCl for VBC−MMA copolymers (100/0, 80/20, 50/50, and 20/80) functionalized with TMMA. (B) Molarity-based distribution coefficients of lanthanide ions in 6 M HCl for VBC−MMA copolymers (100/0, 80/20, 50/50, and 20/80) functionalized with TMMA.

affects the speciation of metal ions and ion exchange then operates by exchanging the chloride ion with the anionic lanthanide complex (Scheme 4).

The results in the high acid region agree with the ion exchange mechanism: the distribution coefficients decrease due to decreasing ion exchange from competition by the high chloride ion concentration.

The proposed schemes are consistent with a report describing the complexation of Tb(III) and Am(III) by *N*,*N*′-dicyclohexyl-*N*,*N*′dimethyltetradecylmalonamide from HNO_3 wherein two modes of complexation were proposed: coordination and ion-pairing (equivalent, in this case, to ion-exchange), each operating at different solution acidities.[33] The extraction of nitric acid when its concentration exceeds 2 M supports the ion-pairing mechanism.

(33) Chan, G. Y. S.; Drew, M. G. B.; Hudson, M. J.; Iveson, P. B.; Liljenzin, J.-O.; Skålberg, M.; Spjuth, L.; Madic, C. *J. Chem. Soc., Dalton Trans.* **1997**, 649–660.

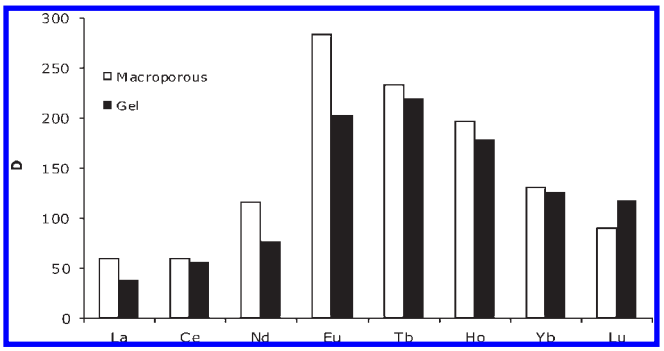

Figure 4. Distribution coefficients of gel and macroporous resins in 6 M HCl.

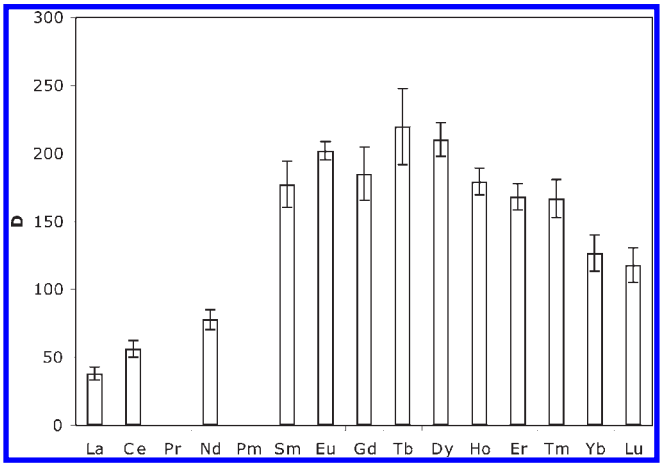

Figure 5. Distribution coefficients of the lanthanide series with TMMA in 6 M HCl.

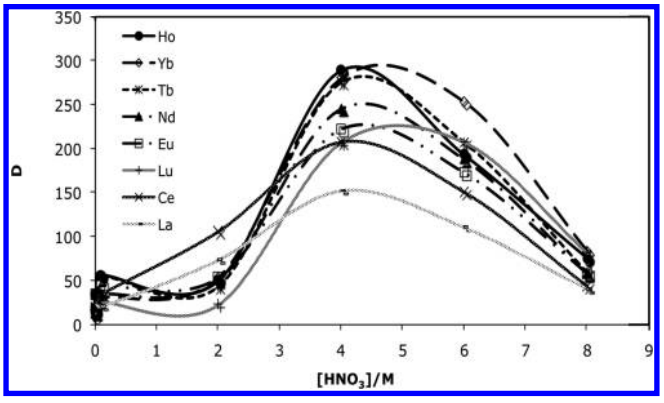

Figure 6. Distribution coefficients for the lanthanides at varying HNO_3 concentrations.

Comparative Study of the Monoamide, Diamide, and Diester Resins. The comparative study summarized in Table 3 is consistent with Scheme 3. The low affinities of the monoamide indicate that protonation of the C=O in the monoamide is not favored in 4 M HCl and only slightly occurs in 6 M HCl. Protonation of the carbonyl oxygen occurs to a much greater extent in the diamide because of the stabilization which results by binding to the neighboring carbonyl,[34] and this results in the iminium nitrogen as the site of ion-exchange. The diester has low affinities, either because there is no protonation of the diester or ion-exchange occurs only at the nitrogen rather than the protonated carbonyl.

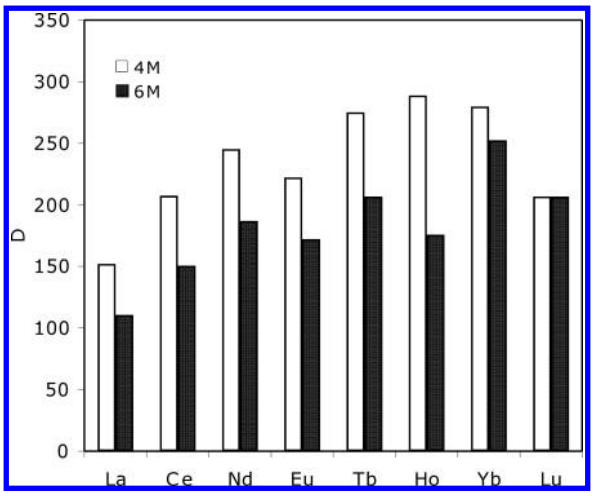

Figure 7. Distribution coefficients of the lanthanides from 4 and 6 M HNO_3.

Effect of HNO_3 Concentration on Lanthanide Affinities. The mechanism of lanthanide complexation from HNO_3 mirrors that from HCl. The decreasing distribution coefficients at higher nitric acid concentrations (Figure 6) is due to the competition between the nitrato complex and the nitrate ion for ion-pairing at the iminium site and formation of the less extractable $Ln(NO_3)_5^{2-}$ species.[35,36] A similar nitric acid dependency has been reported with Cyanex 923 (a mixture of trialkylphosphine oxides) in a solvent extraction study of Am(III):[37] the lanthanide affinities increase with increasing acid concentration and exhibit a peak at 0.75 M HNO_3, followed by a sharp decline as the acid concentration further increases.

Effect of the Counterion on the Complexation of Lanthanides by the TMMA Resin. Similar trends are observed for complexation of the lanthanides by TMMA in HCl and HNO_3 (Figures 1 and 6). The *D* values, however, are greater in HNO_3 than in HCl (Figure 8). This can be attributed to the different solvation properties and hydration energies of the chloride and nitrate ions because binding of a metal complex by a ligand entails at least partial dehydration. The free energy of hydration is higher for nitrate than for chloride (−300 vs −340 kJ/mol, respectively):[38] chloride has the more negative hydration free energy thus making it more difficult to dehydrate the chloro complex in order to bind to the resin, leading to lower affinities.

The importance of the counterion's dehydration energy in determining the extent of complexation was tested by changing the acid to 3 and 6 M H_2SO_4. In both cases, only a low level of complexation was seen for La, Eu, and Lu (Table 4). Sulfate binds lanthanides to form anionic

(34) Ekberg, C.; Enarsson, Å.; Gustavsson, C.; Landgren, A.; Liljenzin, J. O.; Spjuth, L. *Partitioning and Transmutation, Annual report 1999*; Chalmers University of Technology, Göteborg, 1999; ISSN 1402-3091.

(35) Yaita, T.; Ito, D.; Tachimori, S. *J. Phys. Chem. B* **1998**, *102*, 3886–3891.

(36) Abrahamer, I.; Marcus, Y. *J. Inorg. Nucl. Chem.* **1968**, *30*, 1563.

(37) Ansari, S. A.; Murali, M. S.; Pathak, P. N.; Manchanda, V. K. *Solv. Extr. Ion Exch.* **2004**, *22*, 1013–1036.

(38) Marcus, Y. *J. Chem. Soc. Faraday Trans.* **1991**, *87*, 2995–2999.

Scheme 2. Coordination of the Lanthanides by TMMA in Dilute Acid Solutions

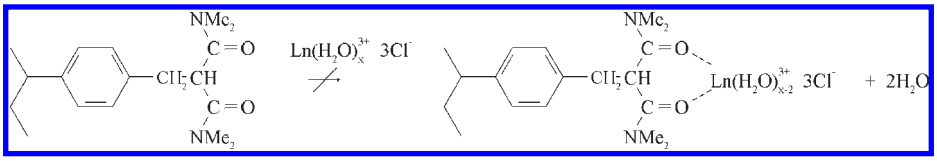

Scheme 3. Protonation of the Malonamide Ligand and Formation of the Iminium Moiety

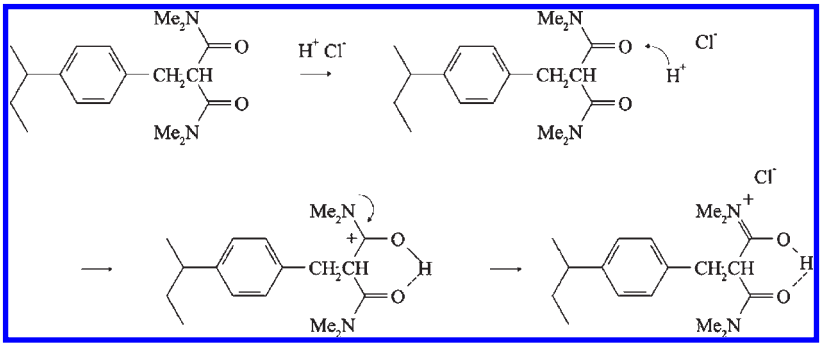

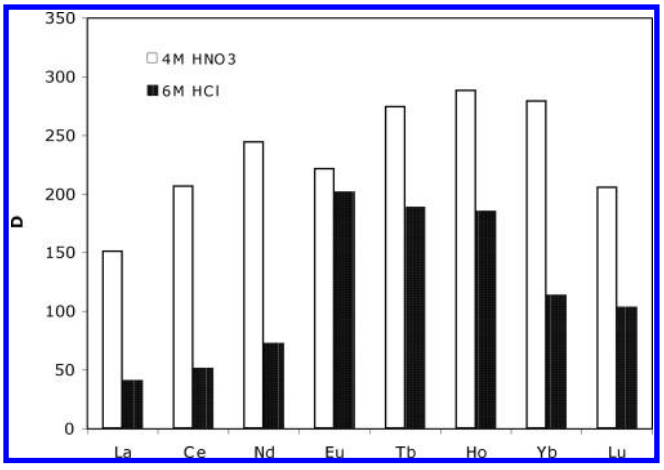

Figure 8. Distribution coefficients of the lanthanides in 4 M HNO_3 and 6 M HCl.

Scheme 4. Ion Exchange of Cl^- at the Iminium Moiety by the Lanthanide Chlorocomplex

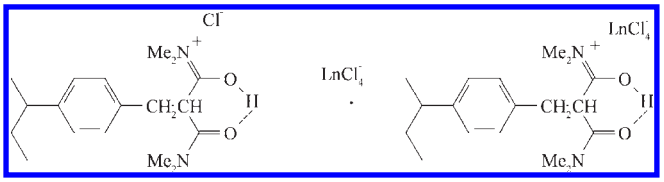

$Ln(H_2O)_x(SO_4)_2^-$ species;[39,40] its hydration energy of −1080 kJ/mol[42] indicates that it is strongly hydrated and thus prefers to remain in aqueous solutions rather than enter the less polar resin.

Mechanism of Recognition. Figure 2 shows that the affinities increase from La to Tb, remain high for Tb and Ho, and then decrease toward Lu. (The affinities in 4 M HNO_3 exhibit a similar trend). Unlike a trend that is monotonic, this bell-shaped trend is not explained by any single property used to characterize the lanthanides: ionic radius, third ionization energy, ionization potential, electronegativity, or hydration energy (Table 5). A continuously increasing or decreasing trend along the series has been reported with polymer-supported complexants with pyridine[41] and sulfonic acid ligands.[42]

Table 4. Distribution Coefficients of Lanthanides Complexed by TMMA from Acidic Solutions

	D					
	H_2SO_4		HCl		HNO_3	
metal	3 M	6 M	4 M	6 M	4 M	6 M
La	13.6	22.8	34.4	42.7	151.9	110.3
Eu	12.4	33.0	114.6	203.3	222.3	172.4
Lu	12.1	34.2	54.1	129.4	206.7	206.9

The current results, in which there is a maximum within the series, is best explained as arising from ionic recognition. Recognition requires two opposing mechanisms that operate on each substrate and a change in trend occurs at the crossover point where the originally dominant mechanism becomes secondary.[43]

Electrostatic attraction is thus one operative mechanism (Scheme 4). The second mechanism is the loss of the waters of hydration (Scheme 5). This occurs upon ion exchange, as observed by neutron diffraction studies of the chloride ion associated with an anion exchange resin,[44] and the lithium ion associated with a cation exchange resin.[45]

The bell-shaped trend results from the increasing electrostatic attraction to the iminium due to the lanthanide

(39) Vercouter, T.; Amekraz, B.; Moulin, C.; Giffaut, E.; Vitorge, P. *Inorg. Chem.* **2005**, *44*, 7570–7581.
(40) Banasal, B. M. L.; Patil, S. K.; Sharma, H. D. *J. Inorg. Nucl. Chem.* **1964**, *26*, 993–1000.
(41) Ikeda, A.; Itoh, K.; Suzuki, T.; Aida, M.; Fujii, Y.; Mitsugashira, T.; Hara, M.; Ozawa, M. *J. Alloys Comp.* **2006**, *408−412*, 1052–1055.
(42) Boyd, G. E. *J. Phys. Chem.* **1978**, *82*, 2704–2709.
(43) Custelcean, R.; Moyer, B. A. *Eur. J. Inorg. Chem.* **2007**, 1321–1340.
(44) Yamanaka, K.; Kameda, Y.; Amo, K.; Usuki, T. *J. Phys. Chem. B* **2007**, *111*, 11337–11341.
(45) Tromp, R. H.; Neilson, G. W. *J. Phys. Chem.* **1996**, *100*, 7380–7383.

Table 5. Physical Properties of the Lanthanides

physical property	La	Ce	Pr	Nd	Pm	Sm	Eu	Gd	Tb	Dy	Ho	Er	Tm	Yb	Lu
Z^a	57	58	59	60	61	62	63	64	65	66	67	68	69	70	71
r^b/Å	1.160	1.143	1.126	1.109		1.079	1.066	1.053	1.040	1.027	1.015	1.004	0.994	0.985	0.977
3rd IP^c/eV	19.18	20.20	21.62	22.10	22.30	23.40	24.92	20.63	21.91	22.8	22.84	22.74	23.68	25.05	20.96
$\sum$IP^d/eV	35.82	36.56	37.62	38.27		40.38	42.95	39.03	30.42	40.66	40.77	40.83	42.04	43.39	40.51
χ^e	1.10	1.12	1.13	1.14		1.17		1.20		1.22	1.23	1.24	1.25		1.27
$-\triangle H_{hyd}{}^d$/ kcal/mol	792.9	805.1	815.3	822.2	830.8	839.6	847.4	853.1	861.3	868.8	876.1	881.8	887.9	893.2	898.8
D_{6MHCl}	38.0	56.2		77.7		172.3	202.1	185.1	219.8	210.4	179.5	168.1	167.0	126.4	117.8

[a] Atomic number. [b] Ionic radius.[48] [c] Third ionization potentials.[49] [d] Ionization potentials.[50] [e] Electronegativity.[51]

Scheme 5. Ion Exchange at the Iminium Moiety Coupled to Lose Some Waters of Hydration

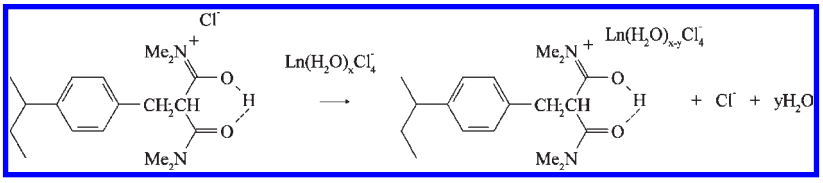

contraction: the increasing positive-charge density on the lanthanide across the series causes it to draw the Cl^- and waters of hydration closer, increasing the overall charge density of the complex and also making ΔH_{hydr} more negative. The increasing electrostatic attraction gives an increasing affinity from La to Tb. As the series passes Tb, ΔH_{hydr} outweighs electrostatic attraction and so precludes the loss of waters of hydration (Scheme 5), thus decreasing the apparent affinity from Dy to Lu.

Increased binding of H_2O to the lanthanides, especially after Eu, has been observed:[46] At low [Cl^-], the hydration numbers of La, Ce, Nd, Eu, and Yb decrease from 9.2 to 8.7 while the Ln−O bond lengths decrease from 2.54 to 2.32 Å, indicating tighter binding of water across the series. In high chloride concentrations (14 M LiCl), chloride incorporation into the inner sphere decreases from La to Eu and, after Eu, there is no chloride and no loss of coordinated water. The decreasing ability of chloride to replace water in the inner sphere across the lanthanide series is consistent with dehydration as the increasingly dominant component of the TMMA−Ln interaction.

The results indicate that an ion exchange mechanism is operative via protonation of the immobilized TMMA carbonyl groups and iminium ion formation. This is supported by studies on TMMA reported in the literature. With soluble molecules, it has been found that the flexibility of TMMA leads to relatively low levels of lanthanide complexation from 1 M HNO_3 when compared to a molecule wherein the diamide structure is incorporated in a rigid 6,6-bicyclic ring.[47] High levels of complexation by the diamide ligand can thus be accomplished by protonation in highly acidic solutions or forcing a cis-dicarbonyl arrangement.

Conclusion

The two opposing mechanisms that operate with TMMA under acidic conditions are electrostatic attraction of the $Ln(H_2O)_xCl_4^-$ or $Ln(H_2O)_x(NO_3)_4^-$ by the protonated ligand and (partial) loss of the waters of hydration as complexation occurs. The key feature in the proposed mechanism is that hydrogen bonding switches on the formation of the iminium group, and it is the site of complexation.

Ionic recognition is operative in the TMMA−Ln interaction under acidic conditions. A variable which distinguishes the current series from other cases wherein there is a linear change in affinity between the ligand and the lanthanides is the ligand itself: a ligand with a moderate affinity is required for ionic recognition to occur; the stronger the ligand, the more it will be able to bind the metal. The strength of the ligand is dependent on its charge density; with the protonated TMMA, the charge density at the iminium site is moderated by the electron-donating methyl groups. Additionally, recognition requires two opposing mechanisms that dominate at different points along a homologous series. The decrease in ionic radius across the lanthanide series acts to increase the electrostatic attraction of the lanthanide complex for the ligand while the increasingly negative hydration enthalpy acts to keep the species in solution. The dominant trend determines the affinity series and the magnitude of the distribution coefficients. Electrostatic attraction dominates from La to Tb giving increasing

(46) Allen, P. G.; Bucher, J. J.; Shuh, D. K.; Edelstein, N. M.; Craig, I. *Inorg. Chem.* **2000**, *39*, 595–601.

(47) Parks, B. W.; Gilbertson, R. D.; Hutchison, J. E.; Healey, E. R.; Weakley, T. J. R.; Rapko, B. M.; Hay, B. P.; Sinkov, S. I.; Broker, G. A.; Rogers, R. D. *Inorg. Chem.* **2006**, *45*, 1498–1507; note added: Preorganization of the diamide ligand in a bicyclic ring may increase its tendency to protonate just as well as it would to chelate, but it is difficult to say conclusively whether protonation would occur in the less acidic solution of a preorganized ligand. However, one of the co-authors of the paper (Dr. Ben Hay) has informed us that the high level of complexation is retained in a solution of 0.1 M HNO_3 + 0.9 M HNO_3, a condition in which protonation is unlikely. The rigidity of the bicyclic diamide might thus favor chelation while the flexibility of the immobilized TMMA ligand might favor protonation and that only from highly acidic (> 4 M) solutions.

(48) Taylor, M. A.; Argirusis, C.; Kilo, M.; Borchardt, G.; Luther, K.-D.; Assums, W. *Solid State Ionics* **2004**, *173*, 51–56.

(49) Cao, X.; Dolg, M. *Chem. Phys. Lett.* **2001**, *349*, 489–495.

(50) Morss, L. R. *J. Phys. Chem.* **1971**, *75*, 392–399.

(51) Barnum, D. W. *Inorg. Chem.* **1983**, *22*, 2297–2305.

distribution coefficients whereas the hydration enthalpy becomes dominant after Tb to give decreasing distribution coefficients. The iminium site must thus be a moderately strong ligand, so that at the midpoint of the lanthanide series, its attraction to the metal is balanced by the metal's attraction to its waters of hydration.

Dehydration of the counterions influences the apparent affinities: The affinities are greater from HNO_3 than HCl and minimal from H_2SO_4. In due course, we will study anion effects by adding alkali metal salts at a constant acid concentration.

The results with TMMA emphasize the importance of hydrogen bonding in affecting ionic affinities. This general effect, which has been observed in our research with phosphorylated polyols, is being incorporated into other amides in order to determine the ionic selectivities of structurally different iminium ions.

Acknowledgment. We gratefully acknowledge support from the U.S. Department of Energy, Office of Basic Energy Sciences, Separations and Analysis Program, through grant DE-FG02-02ER15287.